

# ChemComm

Chemical Communications

Accepted Manuscript

This article can be cited before page numbers have been issued, to do this please use: M. Wu, A. D. Handoko, K. Zhu, L. Chi-Lik Ken, P. Miller, M. R. Crimmin and B. Ramalingam, *Chem. Commun.*, 2025, DOI: 10.1039/D5CC03841C.



This is an Accepted Manuscript, which has been through the Royal Society of Chemistry peer review process and has been accepted for publication.

Accepted Manuscripts are published online shortly after acceptance, before technical editing, formatting and proof reading. Using this free service, authors can make their results available to the community, in citable form, before we publish the edited article. We will replace this Accepted Manuscript with the edited and formatted Advance Article as soon as it is available.

You can find more information about Accepted Manuscripts in the [Information for Authors](#).

Please note that technical editing may introduce minor changes to the text and/or graphics, which may alter content. The journal's standard [Terms & Conditions](#) and the [Ethical guidelines](#) still apply. In no event shall the Royal Society of Chemistry be held responsible for any errors or omissions in this Accepted Manuscript or any consequences arising from the use of any information it contains.

## COMMUNICATION

Electrochemical Dehydrogenative Intramolecular C–C Coupling for Expedient Carbazole Synthesis<sup>†</sup>Mingyue Wu,<sup>a</sup> Albertus Denny Handoko,<sup>a</sup> Kexin Zhu,<sup>b</sup> Chi-Lik Ken Lee,<sup>a</sup> Philip Miller,<sup>b</sup> Mark Crimmin<sup>b</sup> and Balamurugan Ramalingam<sup>\*a,c</sup>Received 00th January 20xx,  
Accepted 00th January 20xx

DOI: 10.1039/x0xx00000x

An electrochemical method for carbazole synthesis via dehydrogenative aryl-aryl coupling of arylamines under metal-free conditions at ambient temperature is presented. The reactivity of arylamines is rationalised by cyclic voltammetry and density functional theory (DFT) studies to provide a preliminary understanding of the observed regioselectivity.

Dehydrogenative aryl-aryl coupling is a powerful strategy for constructing aromatic molecules by directly forming C–C bonds through oxidative processes.<sup>1, 2</sup> Electrochemical dehydrogenative coupling uses the oxidation of suitable aromatic substrates to achieve the dimerisation of aryl units, providing a sustainable alternative to traditional metal-catalysed coupling reactions without chemical oxidants. When two aryl units are connected via a central nitrogen, intramolecular homo-coupling can occur, leading to the formation of carbazoles.<sup>3</sup> Carbazole derivatives are widely used in pharmaceuticals,<sup>4</sup> organic electronics,<sup>5, 6</sup> and functional materials.<sup>7, 8</sup> However, conventional carbazole synthesis often requires multiple reaction steps and suffers from poor atom economy. Thus, the electrochemical dehydrogenative coupling<sup>9</sup> of diphenylamine offers an efficient alternate solution for carbazole synthesis by reducing waste generation. This method eliminates the need for pre-functionalised feedstocks or external oxidants and the use of precious transition-metal catalysts, making it atom-efficient, environmentally benign and cost-effective.

Electrochemical dehydrogenative aryl-aryl coupling has been known for more than a decade, with significant progress reported for the synthesis of biphenols,<sup>10–12</sup> bianilides,<sup>13</sup> meta- and para-terphenyls, as well as cross-coupled products of various heterocycles with phenols.<sup>14–16</sup> However, the

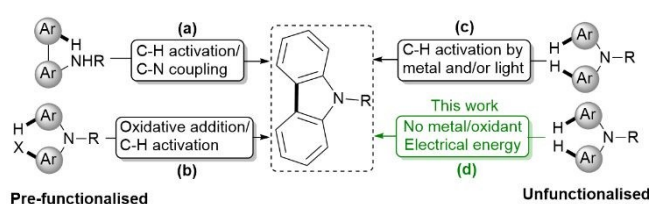


**Fig. 1.** Current attractive strategies (a–c) for the synthesis of carbazoles compared to our sustainable approach (d). Existing strategies (a–c) rely on metal catalysts or oxidants and require pre-functionalized substrates. In contrast, our sustainable approach (d) uses only electricity to achieve oxidative coupling of aryl groups at room temperature, eliminating the need for oxidants or metal catalysts.

electrochemical dehydrogenative strategy has not been utilised on substrates that are pre-functionalised for carbazole synthesis. Transition metal-catalysed synthesis of carbazoles, involving oxidative pathways has become increasingly attractive to conventional synthesis.<sup>17–19</sup> Three major approaches (Fig. 1) have been reported for the synthesis of carbazoles adopting novel methodologies, (i) concerted C–H activation of pre-functionalised bi-aryl amines and subsequent C–N bond formation via either amination ( $R = H, \text{alkyl}, \text{Bn}$ )<sup>20</sup> or amidation ( $R = \text{acetyl}$ )<sup>21–23</sup> using metal catalysts or electrochemical dehydrogenative coupling (Fig. 1a);<sup>24</sup> (ii) oxidative addition of aryl halides to metal catalysts followed by C–H activation (Fig. 1b);<sup>25–30</sup> (iii) Intramolecular oxidative C–H/C–H coupling (Fig. 1c),<sup>31, 32</sup> which can proceed in the presence of a metal catalyst or under photoredox conditions (e.g., using  $\text{Fe}^{33}$  or  $\text{Cu}^{34}$ -based catalysts) with iodine or molecular oxygen as the oxidant. While the above approaches are applicable to broad substrate scope, the need for pre-functionalisation with either amine or halogen and the reliance on precious metals for substrate activation are disadvantageous. From a sustainability standpoint, metal-free strategies in organic synthesis are especially attractive compared to methods that depend on precious metal catalysis.

To the best of our knowledge, neither simple nor substituted carbazoles have been synthesised from diaryl- or triaryl- amines via anodic oxidation without the use of oxidants or metals or photoredox catalysts. Notably, Beil et al.<sup>35</sup> reported oxidative coupling using an active molybdenum anode under a constant current density of  $7.5 \text{ mA cm}^{-2}$ . Under these

<sup>a</sup> Institute of Sustainability for Chemicals, Energy and Environment (ISCE<sup>2</sup>), Agency for Science, Technology and Research (A\*STAR), 1 Pesek Road, Singapore 627833, Republic of Singapore. E-mail: balamurugan\_ramalingam@isce2.a-star.edu.sg

<sup>b</sup> Molecular Sciences Research Hub, Department of Chemistry, Imperial College London, London, W12 0BZ, UK.

<sup>c</sup> Institute of Materials Research and Engineering (IMRE), Agency for Science Technology and Research (A\*STAR), Singapore 138634, Republic of Singapore

<sup>†</sup> Electronic supplementary information (ESI) available. See DOI: 10.1039/x0xx00000x



conditions, the formation of six- or seven-membered rings was favoured achieving isolated yields of up to 80%. It was proposed that  $[\text{Mo}(\text{OCH}(\text{CF}_3)_2)_5]$ , generated in the reaction medium, played a key role in promoting oxidative coupling. Nevertheless, the formation of carbazoles was limited to a yield of only 10%, and the synthesis of other five-membered rings remained challenging, with yields reaching up to 31%. Herein, we report an electrochemical method for carbazole synthesis carried out at room temperature, without the use of metal catalysts or external oxidants. This environmentally benign approach allows direct C–C bond formation without use of metal catalyst. Furthermore, this study offers valuable insights into the underlying reaction pathways for the selective formation of carbazoles.

Electrochemical oxidation of tris(3,4-dimethoxyphenyl)amine (**A1**) was initiated in a two-electrode setup under galvanostatic control. A detailed optimisation study is presented in Table S1 (Supplementary Information). The optimal conditions were then applied to various tertiary amines to explore the homo-aryl coupling reaction scope (Fig. 2). Highly electron-rich substrates like **A1** can undergo oxidation readily, affording the desired carbazole **C1** in 85% isolated yield. Replacing one of the OMe groups by a Me group as in **C2** or 3,4-dimethoxyphenyl moiety by phenyl (**C3**) decreased the yield substantially. Replacing electron-rich aryl rings of the tertiary aryl amine with a *p*-halo-substituted phenyl group did not significantly impact the

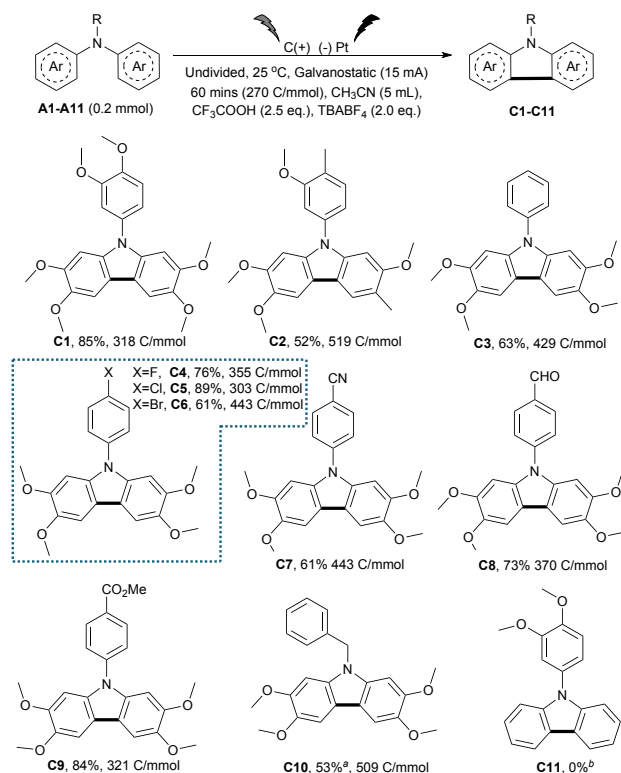


**Fig. 2** Efficiency of electrochemical dehydrogenative coupling of tertiary amines. Isolated yields are reported. Refer to SI for the synthesis of starting materials (**A1**–**A11**) and the corresponding products (**C1**–**C11**) and analytical data. <sup>a</sup>In the presence of 10 mol % of ferrocene as a mediator. <sup>b</sup>Possible formation of dimerization product (**C11-dimer**, 38%) was observed (cf. supplementary information Section 6)

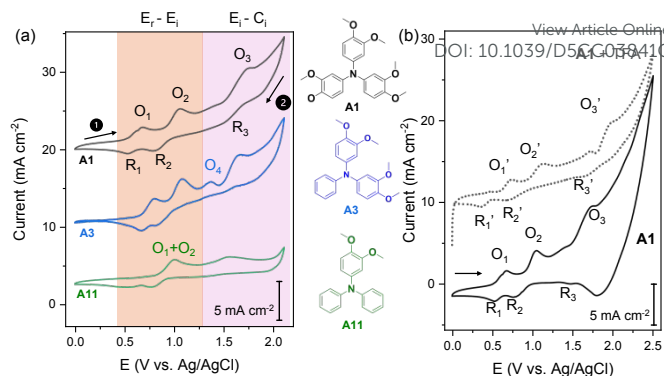


**Fig. 3** Cyclic voltammetry (CV) was performed on mirror polished glassy carbon working electrode ( $\approx 0.071 \text{ cm}^2$ ), platinum counter ( $\approx 2 \text{ cm}^2$ ), and leakless Ag/AgCl reference electrode under the optimised reaction conditions described in Fig. 2 but with larger total volume of 10 mL. (a) Cyclic voltammetry (CV) of **A1**, **A3** and **A11** at scan rate 10 mV s<sup>-1</sup> vs. Ag/AgCl. (b) CV of **A1** before (solid line) and after TEA addition (dotted lines).

product yields, affording carbazoles **C4**–**C6** in 61–89% yield. Notably, no dehalogenation or direct arylation of products was observed, which is one of the possible side reactions in metal-catalysed coupling reactions. Functional groups such as  $-\text{CN}$  (**C7**),  $-\text{CHO}$  (**C8**) and  $-\text{CO}_2\text{Me}$  (**C9**) were unaffected under the electrooxidation conditions and provided the coupling products in good to excellent yields (61–84%). Notably, the stepwise replacement of the 3,4-dimethoxyphenyl groups with unsubstituted phenyl rings had a marked effect on the yields of **C3** (63%) and **C11** (0%). The optimised methodology appears to perform well with electron-rich substrates, and we believe there is significant potential to extend its applicability to electron-deficient substrates by fine-tuning the electrochemical conditions and by suppressing side reactions.

To understand the reactivity differences amongst substrates, cyclic voltammetry (CV) examinations were performed on **A1**, **A3**, and **A11** under the same reaction conditions using a potentiostat (Gamry Reference 600+). Three oxidation and reduction event pairs were detected respectively on **A1** upon the first anodic and return cathodic scan (Fig. 3a).  $\text{O}_1/\text{R}_1$  pair displayed relatively symmetrical peak area ratio of  $\approx 0.91$  and moderate peak-to-peak separation ( $\Delta E_p$ ) of  $\approx 157 \text{ mV}$ , indicative of a (quasi)reversible single electron transfer process ( $E_1$ ).<sup>36</sup> Although the  $\Delta E_p$  is wider than the theoretical value of 60 mV, it is comparable to a  $\text{Fc}/\text{Fc}^+$  reference ( $\Delta E_p \approx 120 \text{ mV}$ , Fig. S2a), suggesting significant influence from iR drop or passivation that widens  $\Delta E_p$ .  $\text{O}_2/\text{R}_2$  shows a more irreversible single electron transfer behaviour ( $E_i$ ) with larger peak area ratio of  $\approx 1.26$  and wider  $\Delta E_p$  of  $\approx 278 \text{ mV}$ . Distinct from the rest, the  $\text{O}_3/\text{R}_3$  pair is unsymmetrical, with very large area ratio of  $>30$  and  $\Delta E_p$  of  $\approx 257 \text{ mV}$ , indicative of a two-step reaction consisting of irreversible electron transfer followed by irreversible chemical reaction ( $E_1$ – $\text{C}_1$ ). As the oxidative coupling process of **A1** to yield **C1** is expected to involve 2 e<sup>-</sup> transfer, we hypothesise that the relevant coupling process is reflected by  $\text{O}_1$  and  $\text{O}_2$ , while  $\text{O}_3$  may be linked to overoxidation that could lead to possible side-reactions decreasing the efficiency of the coupling reaction.<sup>37</sup> Our position is supported by chronopotentiometric measurements of **A1** at 10 and 15 mA (5.6 and 8.5 mA cm<sup>-2</sup>



respectively, Fig. S4), where poor **C1** yield (12%) at 10 mA applied current (Table S1, entry 5) can be rationalised to the insufficient voltage ( $\approx 0.7$  V max) to reach  $O_2$  oxidation event.

Comparing the redox behaviour of different substrates,  $O_1$  and  $O_2$  peaks are 12–16 mV more anodic on **A3** (Fig. 3a), suggesting that the oxidative coupling of the latter is more arduous. **A3** also displays similar  $O_3$  potential to **A1**. However, a new irreversible oxidation peak  $O_4$  was detected at 1.46 V, earlier than  $O_3$ . This suggests that **A3** may have additional overoxidation mechanisms that can adversely affected **C3** yield (63%). The redox behaviour of **A11** (Fig. 3a) is rather different, with only two oxidation events  $O_5$  and  $O_3$  observed in the potential range of CV. As reduction events  $R_1$  and  $R_2$  are still present around 0.50 and 0.76 V, we deduced that reduction event  $O_5$  may represent merged  $O_1$  and  $O_2$  components. The position of  $O_5$  peak is at least 320 mV more anodic compared to  $O_1$  in **A1**, suggesting that the oxidative coupling process on **A11** is more challenging. At the same time,  $O_3$  peak appears 250 mV earlier compared to **A1**, suggesting more facile overoxidation. We believe that the combination of these factors might lead to the formation of a possible dimeric product **C11-dimer** (cf. Supplementary Information Section 6) rather than the expected **C11**.

Next, the role of TFA additive can be elucidated by comparing the CV of **A1** with and without TFA (Fig. 3b). With TFA addition, the most notable change in the redox behaviour of **A1** is the anodic shift of  $O_3$  peak to  $O_3'$  from 1.76 to 1.96 V, while the position of  $O_1'$  and  $O_2'$  are relatively unchanged from  $O_1$  and  $O_2$ , barring 4–6 mV shift. Thus, we posit that the TFA addition did not actually make the oxidative coupling of **A1** easier, but rather, it makes the over-oxidation event more difficult through protonation of the central N atom. Thus, a more stable **A1** (or **C1**) would allow the current controlled coupling process to proceed with a wider electrochemical stability window. This hypothesis is corroborated by significantly ( $\approx 5.9\times$ ) steeper yield growth compared to conversion growth with more TFA added (Fig. S4, Supplementary Information). A relatively strong and electrochemically stable acid is required for this scheme, as our attempt to substitute TFA with acetic acid (Table S1, entry 10) did not improve **C1** yield. On the other hand, more acidic methanesulfonic acid (Table S1, entry 8) appears to improve **C1** yield slightly but not as good as TFA, possibly because of better oxidation stability of TFA.<sup>38</sup>

In the electrochemical oxidation process, we observed the favourable formation of  $C_6-C_6'$  coupling products of carbazole. A plausible reaction pathway for the formation of carbazole product **C1** is proposed in Fig. S9. To gain insight into the electronic and structural properties underlying the electrochemical dehydrogenative C–C coupling reaction, we employed density functional theory (DFT) calculations. These calculations focused on the relative energies of isomeric forms of the products and electronic structure of potential reaction intermediates. The Gibbs free energies of three possible oxidation products formed through coupling at the  $C_2-C_2'$ ,  $C_2-C_6'$ , and  $C_6-C_6'$  carbon atoms of **A1** (Fig. 4a). A series of possible

conformers for each product was identified based on the relative orientation of the methoxy groups with respect to their attached phenyl rings. The DFT analysis reveals that among the various conformations, the lowest-energy structure corresponds to the  $C_6-C_6'$  coupled product, which is thermodynamically more stable by 0.5 kcal mol<sup>-1</sup> compared to the  $C_2-C_6'$  product and by 6.0 kcal mol<sup>-1</sup> compared to the  $C_2-C_2'$  product. These data suggest that the selectivity of the reaction is determined by the low kinetic barrier to form the experimentally observed  $C_6-C_6'$  product rather than thermodynamics.

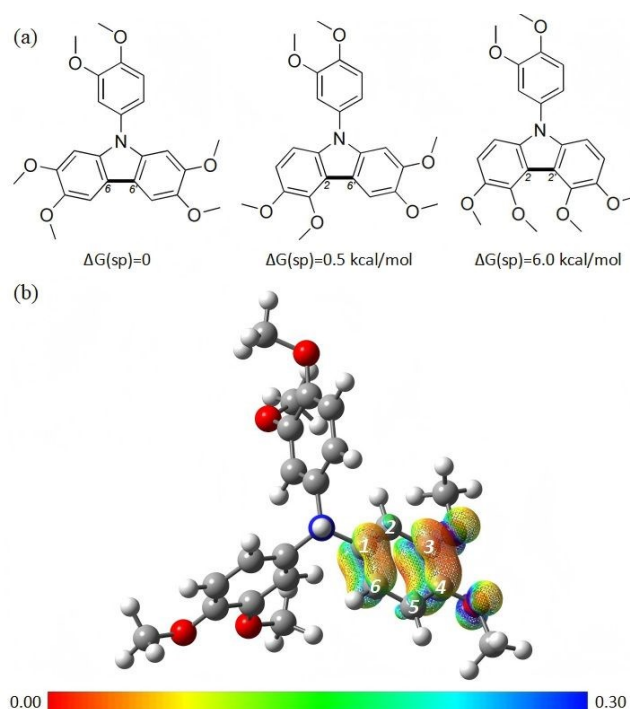


**Fig. 4.** DFT calculations were carried out with Gaussian 16 (Revision C.02). Geometry optimisation was performed using the  $\omega$ B97X-D functional including geometrical dispersion corrections described by Grimme's D2 correction. (a) Structures of three different optimised isomers of **C1** (from left to right  $C_6-C_6'$ ,  $C_2-C_2'$ , and  $C_2-C_6'$ ). (b) Spin density distribution of  $^2[\mathbf{A1-H}]^{2+}$ .

To gain further insight into the electronic properties of potential reaction intermediates, the structures of the radical cation  $^2[\mathbf{A1}]^+$  and its protonated analogue  $^2[\mathbf{A1-H}]^{2+}$  were calculated defining each as doublet spin state ( $S = 1/2$ ). Given the experimental reaction conditions and high concentration of TFA, it is likely that the substrate exists in its protonated form in solution and  $^2[\mathbf{A1-H}]^{2+}$  is a plausible intermediate following electrochemical oxidation of  $[\mathbf{A1-H}]^+$ . Examination of the spin-density plot of  $^2[\mathbf{A1-H}]^{2+}$  (Fig. 4b) shows that the unpaired electron's spin is confined within just one of the aryl rings. While delocalised, there is spin-density on  $C_6$  position, suggesting that this site should possess radical character and thereby supporting the experimentally observed site of reactivity.

In summary, this study presents an electrochemical approach for synthesising carbazoles via intramolecular dehydrogenative aryl–aryl coupling of arylamines. The methodology offers significant advantages in terms of atom economy, eliminating the need for precious metal catalysts, stoichiometric oxidants, or pre-functionalised starting materials. Trifluoroacetic acid





(TFA) was identified as a critical additive, increasing the yield of **C1** from 29% to 87% by expanding the electrochemical stability window and suppressing undesired overoxidation. The method afforded good to excellent yields (61–90%) across a range of electron-rich and para-halo-substituted substrates, whereas less electron-donating groups led to a marked decrease in efficiency. The reaction exhibited complete regioselectivity, consistently yielding the C<sub>6</sub>–C<sub>6</sub>' coupled product. DFT calculations supported the experimental observations, showing the observed product is the thermodynamically most stable isomer and is also likely kinetically favoured based on the electronic structure of the possible radical intermediate. Overall, this work establishes a practical and mechanistically informed method for carbazole synthesis and contributes to the advancement of methodologies in electro-organic synthesis. We are currently focusing on expanding the new methodology for the construction of oxygen- and sulphur-containing heterocycles, as well as the synthesis of carbazole-containing natural products.

This work was funded by the Horizontal Technology Coordinating Office (HTCO), Agency for Science, Technology and Research (A\*STAR), Singapore, under project number C231218004. B,R acknowledges Materials Generative Design and Testing Framework (MAT-GDT) Program at A\*STAR (Grant No. M24N4b0034) for the support.

## Conflicts of interest

There are no conflicts to declare.

## Data availability

Data for this article has been included as a part of the ESI.†

## Notes and references

- J. L. Röckl, D. Pollok, R. Franke and S. R. Waldvogel, *Acc. Chem. Res.*, 2020, **53**, 45–61.
- Y. Yuan and A. Lei, *Acc. Chem. Res.*, 2019, **52**, 3309–3324.
- L. A. T. Allen and P. Natho, *Org. Biomol. Chem.*, 2023, **21**, 8956–8974.
- A. Caruso, J. Ceramella, D. Iacopetta, C. Saturnino, M. V. Mauro, R. Bruno, S. Aquaro and M. S. Sinicropi, *Molecules*, 2019, **24**, 1912.
- Y. Liu, Y. Sun, M. Li, H. Feng, W. Ni, H. Zhang, X. Wan and Y. Chen, *RSC Adv.*, 2018, **8**, 4867–4871.
- M. Li, W. Ni, H. Feng, X. Wan, Y. Liu, Y. Zuo, B. Kan, Q. Zhang and Y. Chen, *Org. Electron.*, 2015, **24**, 89–95.
- X.-D. Yuan, J. Liang, Y.-C. He, Q. Li, C. Zhong, Z.-Q. Jiang and L.-S. Liao, *J. Mater. Chem. C*, 2014, **2**, 6387.
- D. Magaldi, M. Ulfa, S. Peralta, F. Goubard, T. Pauporté and T.-T. Bui, *J. Mater. Sci. Mater. Electron.*, 2021, **32**, 12856–12861.
- A. B. Dapkekar, J. Naveen and G. Satyanarayana, *Asian J. Org. Chem.*, 2025, **14**, e202500324.
- B. Dahms, P. J. Kohlpaintner, A. Wiebe, R. Breinbauer, D. Schollmeyer and S. R. Waldvogel, *Chem. Eur. J.*, 2019, **25**, 2713–2716.
- B. Elsler, D. Schollmeyer, K. M. Dyballa, R. Franke and S. R. Waldvogel, *Angew. Chem. Int. Ed.*, 2014, **53**, 5210–5213.
- B. Elsler, A. Wiebe, D. Schollmeyer, K. M. Dyballa, R. Franke and S. R. Waldvogel, *Chem. Eur. J.*, 2015, **21**, 12321–12325.
- L. Schulz, M. Enders, B. Elsler, D. Schollmeyer, K. M. Dyballa, R. Franke and S. R. Waldvogel, *Angew. Chem. Int. Ed.*, 2017, **56**, 4877–4881.
- A. Wiebe, S. Lips, D. Schollmeyer, R. Franke and S. R. Waldvogel, *Angew. Chem. Int. Ed.*, 2017, **56**, 14727–14731.
- S. Lips, D. Schollmeyer, R. Franke and S. R. Waldvogel, *Angew. Chem. Int. Ed.*, 2018, **57**, 13325–13329.
- S. Lips, B. A. Frontana - Uribe, M. Dörr, D. Schollmeyer, R. Franke and S. R. Waldvogel, *Chem. Eur. J.*, 2018, **24**, 6057–6061.
- D.-Y. Goo and S. K. Woo, *Org. Biomol. Chem.*, 2016, **14**, 122–130.
- T. Watanabe, S. Oishi, N. Fujii and H. Ohno, *J. Org. Chem.*, 2009, **74**, 4720–4726.
- St. Jean, David J., S. F. Poon and J. L. Schwarzbach, *Org. Lett.*, 2007, **9**, 4893–4896.
- J. A. Jordan-Hore, C. C. C. Johansson, M. Gulias, E. M. Beck and M. J. Gaunt, *J. Am. Chem. Soc.*, 2008, **130**, 16184–16186.
- W. C. P. Tsang, N. Zheng and S. L. Buchwald, *J. Am. Chem. Soc.*, 2005, **127**, 14560–14561.
- S. H. Cho, J. Yoon and S. Chang, *J. Am. Chem. Soc.*, 2011, **133**, 5996–6005.
- W. C. P. Tsang, R. H. Munday, G. Brasche, N. Zheng and S. L. Buchwald, *J. Org. Chem.*, 2008, **73**, 7603–7610.
- A. Kehl, N. Schupp, V. M. Breising, D. Schollmeyer and S. R. Waldvogel, *Chem. Eur. J.*, 2020, **26**, 15847–15851.
- R. B. Bedford and C. S. J. Cazin, *Chem. Commun.*, 2002, DOI: 10.1039/B207712B, 2310–2311.
- K. K. Gruner and H.-J. Knölker, *Org. Biomol. Chem.*, 2008, **6**, 3902–3904.
- D. Tselikhovsky and S. L. Buchwald, *J. Am. Chem. Soc.*, 2010, **132**, 14048–14051.
- A. Khan, R. Karim, H. Dhimane and S. Alam, *ChemistrySelect*, 2019, **4**, 6598–6605.
- Y. Tanji, N. Mitsutake, T. Fujihara and Y. Tsuji, *Angew. Chem. Int. Ed.*, 2018, **57**, 10314–10317.
- L.-C. Campeau, M. Parisien, A. Jean and K. Fagnou, *J. Am. Chem. Soc.*, 2006, **128**, 581–590.
- G. Brufani, S. Chen, B. Di Erasmo, A. Afanasenko, Y. Gu, C.-J. Li and L. Vaccaro, *ACS Sustain. Chem. Eng.*, 2024, **12**, 8562–8572.
- S. Trosien, P. Böttger and S. R. Waldvogel, *Org. Lett.*, 2014, **16**, 402–405.
- S. Parisien-Collette, A. C. Hernandez-Perez and S. K. Collins, *Org. Lett.*, 2016, **18**, 4994–4997.
- A. C. Hernandez - Perez and S. K. Collins, *Angew. Chem. Int. Ed.*, 2013, **52**, 12696–12700.
- S. B. Beil, T. Müller, S. B. Sillart, P. Franzmann, A. Bomm, M. Holtkamp, U. Karst, W. Schade and S. R. Waldvogel, *Angew. Chem. Int. Ed.*, 2018, **57**, 2450–2454.
- R. S. Nicholson, *Anal. Chem.*, 1965, **37**, 1351–1355.
- K. Karon and M. Lapkowski, *J. Solid State Electrochem.*, 2015, **19**, 2601–2610.
- C. Depecker, H. Marzouk, S. P. Trevin and J. Devynck, *New J. Chem.*, 1999, **23**, 739–742.



Data for this article has been included as a part of the ESI.†

[View Article Online](#)  
DOI: 10.1039/D5CC03841C